Neuron dynamics variability and anomalous phase synchronization of neural networks

B. R. R. Boaretto, R. C. Budzinski, T. L. Prado, Jürgen Kurths, and S. R. Lopes

Citation: Chaos **28**, 106304 (2018); doi: 10.1063/1.5023878
View online: https://doi.org/10.1063/1.5023878
View Table of Contents: http://aip.scitation.org/toc/cha/28/10
Published by the American Institute of Physics

Neuron dynamics variability and anomalous phase synchronization of neural networks

B. R. R. Boaretto,[1] R. C. Budzinski,[1] T. L. Prado,[2] Jürgen Kurths,[3,4] and S. R. Lopes[1,3,4,a)]
[1]*Departamento de Física, Universidade Federal do Paraná, 81531-980 Curitiba, Brazil*
[2]*Instituto de Engenharia, Ciência e Tecnologia, Universidade Federal dos Vales do Jequitinhonha e Mucuri, 39440-000 Janaúba, Brazil*
[3]*Potsdam Institute for Climate Impact Research - Telegraphenberg A 31, 14473 Potsdam, Germany*
[4]*Department of Physics, Humboldt University Berlin, 12489 Berlin, Germany*

(Received 29 January 2018; accepted 5 July 2018; published online 5 October 2018)

Anomalous phase synchronization describes a synchronization phenomenon occurring even for the weakly coupled network and characterized by a non-monotonous dependence of the synchronization strength on the coupling strength. Its existence may support a theoretical framework to some neurological diseases, such as Parkinson's and some episodes of seizure behavior generated by epilepsy. Despite the success of controlling or suppressing the anomalous phase synchronization in neural networks applying external perturbations or inducing ambient changes, the origin of the anomalous phase synchronization as well as the mechanisms behind the suppression is not completely known. Here, we consider networks composed of $N = 2000$ coupled neurons in a small-world topology for two well known neuron models, namely, the Hodgkin-Huxley-like and the Hindmarsh-Rose models, both displaying the anomalous phase synchronization regime. We show that the anomalous phase synchronization may be related to the individual behavior of the coupled neurons; particularly, we identify a strong correlation between the behavior of the inter-bursting-intervals of the neurons, what we call neuron variability, to the ability of the network to depict anomalous phase synchronization. We corroborate the ideas showing that external perturbations or ambient parameter changes that eliminate anomalous phase synchronization and at the same time promote small changes in the individual dynamics of the neurons, such that an increasing individual variability of neurons implies a decrease of anomalous phase synchronization. Finally, we demonstrate that this effect can be quantified using a well known recurrence quantifier, the "determinism." Moreover, the results obtained by the determinism are based on only the mean field potential of the network, turning these measures more suitable to be used in experimental situations. *Published by AIP Publishing.* https://doi.org/10.1063/1.5023878

Neural phase synchronization (PS) is one of the most important problems in neural systems since it is related to how information is processed in the brain. A large number of works focus on how the connectivity structure (which, in general, is neither random nor regular) of a network is related to PS. It is known that some neural (sub)networks in the brain have small-world properties, allowing a short mean path length and at the same time a large clustering coefficient. PS occurring even for weak coupling and under small-world regimes may be related to a disorder of the nervous system, like Parkinson's disease. In this paper, we aim at studying how anomalous PS phenomenon of small-world networks composed of bursting HodgkinHuxley-type and HindmarshRose neuron models are related to the individual behavior of the neurons. To perform the analysis, we use the Kuramoto order parameter and the recurrence quantifier, the so called "determinism." The determinism is computed using just the mean field potential of the network and leads to similar results to those obtained using the order parameter that must be computed based on the signal of each neuron on the networks.

a)lopes@fisica.ufpr.br

I. INTRODUCTION

Phase synchronization of chaotic systems has been extensively studied in the last few decades since the phenomenon has been discovered in nature in several situations, including coupled networks.[1–4] Particularly important is the dynamic behavior of firing neuron networks that display a great variability of phenomena, including distinct forms of PS.[5–8] In many situations, a synchronized network must be avoided, as it is the case of Parkinson's disease, where in some situations excessive phase synchronization is associated with the oscillatory activity in the beta frequency band (around 20 Hz) in the basal ganglia and other parts of the brain,[9] or due to epilepsy, where episodes of seizures are characterized by complex relationships between synchronization and anomalous synchronization of neurons[10] since epileptic seizures increase coherence of neurons as well as the synchronization throughout the network.[11]

PS processes in networks are closely related to the topology of the connections, and the study of the connection matrix properties is largely used to promote understanding of the PS mechanisms. In a healthy human brain, for example, $N \approx 10^{11}$ neuron cells are organized in sub-areas, each area having its specified function and individual neuron dynamics.[12]

The neurons are interconnected through $n \approx 10^{15}$ synapses,[13] performing a complex network of networks. Mathematically, these networks are often represented by a reduced set of nodes (neurons) connected to each other by edges (synapses) forming a smaller, but still complex networks.[14] Distinct topologies of connections have been considered for computer generated neural networks, such as small-world, scale-free, and random schemes.[15–19]

The collective dynamic behavior of a neural network also depends on the individual action of the neurons which in general have two distinct dynamic patterns of the action potential. The first one is known as spike regime and can be understood as a single and recurrent firing. The second one is a burst regime, which is characterized by a sequence of spikes followed by quiescent periods. The dynamics of the bursting behavior can be understood by considering two time scales, a fast one related to spiking activity and a slow one, which is associated with bursting activity itself.[6] The existence of a slow time scale enables us to define a bursting phase and a frequency of bursting for each neuron in the network, such that the existence of coherent bursting neurons can be understood as a PS of the network.[6,8,20] Sometimes, in real data it is not possible to observe a sharp boundary between spiking and bursting since changes of applied currents in Eq. (1) can transform gradually bursting to spiking regimes. In experimental recordings, it is not uncommon to observe both bursting and individual spikes in the same neural unit.[21,22]

In this work, we consider models of $N = 2000$ bursting neurons under small-world topology since this kind of connection architecture generates appropriate neural networks with a large clustering, thanks to the local connections, and a short mean path length, thanks to the non-local connections which act as shortcuts in the system.[14,15] This topology is usually found in real neural system,[23,24] so we adopted the Newman-Watts route[25] to build small-world networks where the regular part of the networks consists in connections between second-neighbors and the non-local connection probability is fixed in $p = 0.001$ creating ≈ 2000 shortcuts on the network.

We study the relation between individual dynamic behaviors of neurons and the collective dynamics depicted by weakly coupled networks where anomalous PS has been reported.[26–28] We use two distinct neuron models: the first one consists on a variation of the Hodgkin-Huxley model[29] with the addition of parameters that depend on the temperature of the neurons, also including two slow ionic currents related to calcium ion[30] known as a thermally sensitive Hodgkin-Huxley model.[31] The second one is the Hindmarsh-Rose model,[32] which is a set of three differential equations in which a bursting behavior can be observed.

We propose that the presence of PS regime characterized by a non-monotonous dependence of the PS level on the coupling strength and occurring for weak coupling regime (what we call anomalous PS) is related (not exclusively) to the individual behavior of each neuron. Particularly, we show evidence that a low variability of the inter-burst intervals of neurons implies the emergence of this regime of PS of the network. As the variability grows, the anomalous PS diminishes, such that for a large enough variability, the network displays no anomalous PS and behaves similarly to a set of coupled Kuramoto oscillators, concerning the PS process as the coupling parameter is increased.[2]

The paper is organized as follows. In Sec. II, we present details of the neuron models used and its connection schemes. In Sec. III, we introduce how PS is quantified using recurrence analysis and Kuramoto order parameter. In Sec. IV, we show results identifying the inter-dependency relation of the anomalous PS on the individual behavior of the neurons. Our conclusions are in the last section.

II. NEURON MODELS

A thermally sensitive Hodgkin-Huxley (H-H) model[31] is an adaptive H-H model,[29] where the dynamics varies according to the temperature. The model consists of six differential equations describing the dynamics in time of the membrane potential of each neuron, $V_i(t)$ as a function of the current density through the cell membranes,

$$C_{\mathrm{m}}\frac{dV_i}{dt} = -J_{i,\mathrm{Na}} - J_{i,\mathrm{K}} - J_{i,\mathrm{sd}} - J_{i,\mathrm{sa}} - J_{i,\mathrm{L}} + J_{i,\mathrm{coup}}, \quad (1)$$

where V_i is measured in mV and considered as the fast variable of the model, C_{m} is the specific membrane capacitance (μF/cm^2), $J_{i,\mathrm{Na}}$, $J_{i,\mathrm{K}}$, and $J_{i,\mathrm{L}}$ are the sodium, potassium, and non-gated channels density (specific) currents, measured in μA/cm^2. The terms added by Braun *et al.*[31], $J_{i,sd}$ and $J_{i,sa}$ are slow density (specific) currents measured in μA/cm^2, and are related to the depolarization and hyper-polarization oscillations, respectively. The former current densities promote a slower activation of the neurons cells for low membrane potentials and the interplay between fast and slow dynamics leads to a bursting.[31]

The time evolution of the specific currents composing the thermally sensitive neuron model[31] is described in terms of the Nernst's potential of each ion and leak channels by

$$J_{i,\mathrm{Na}} = \rho\overline{g}_{\mathrm{Na}}\alpha_{i,\mathrm{Na}}(V_i - E_{\mathrm{Na}}), \quad (2)$$

$$J_{i,\mathrm{K}} = \rho\overline{g}_{\mathrm{K}}\alpha_{i,\mathrm{K}}(V_i - E_{\mathrm{K}}), \quad (3)$$

$$J_{i,\mathrm{sd}} = \rho\overline{g}_{\mathrm{sd}}\alpha_{i,\mathrm{sd}}(V_i - E_{\mathrm{sd}}), \quad (4)$$

$$J_{i,\mathrm{sa}} = \rho\overline{g}_{\mathrm{sa}}\alpha_{i,\mathrm{sa}}(V_i - E_{\mathrm{sa}}), \quad (5)$$

$$J_{i,\mathrm{L}} = \overline{g}_{\mathrm{L}}(V_i - E_{\mathrm{L}}), \quad (6)$$

where E_{Na}, E_{K}, E_{sd}, E_{sa}, and E_{L} are the Nernst's potentials for each specific current, measured in mV and $\overline{g}_{\mathrm{Na}}$, $\overline{g}_{\mathrm{K}}$, $\overline{g}_{\mathrm{sd}}$, $\overline{g}_{\mathrm{sa}}$, and $\overline{g}_{\mathrm{L}}$ are maximum (specific) conductances, measured in mS/cm^2. The term ρ denotes one of the temperature dependence of the model and it is described by

$$\rho = \rho_0^{(T-T_0)/\tau_0}, \quad (7)$$

where ρ_0, T_0, and τ_0 are constants. Following the original model,[31] a possible temperature dependence in Eq. (6) is not considered due to the smaller temperature dependence of leak channels compared to ion channels.[33]

The terms $\alpha_{i,\mathrm{Na}}$, $\alpha_{i,\mathrm{K}}$, $\alpha_{i,\mathrm{sd}}$, and $\alpha_{i,\mathrm{sa}}$ are related to the activation of channels and their temporal evolutions are described

by

$$\frac{d\alpha_{i,\mathrm{Na}}}{dt} = \frac{\phi}{\tau_{\mathrm{Na}}}(\alpha_{i,\mathrm{Na},\infty} - \alpha_{i,\mathrm{Na}}), \tag{8}$$

$$n\frac{d\alpha_{i,\mathrm{K}}}{dt} = \frac{\phi}{\tau_{\mathrm{K}}}(\alpha_{i,\mathrm{K},\infty} - \alpha_{i,\mathrm{K}}), \tag{9}$$

$$\frac{d\alpha_{i,\mathrm{sd}}}{dt} = \frac{\phi}{\tau_{\mathrm{sd}}}(\alpha_{i,\mathrm{sd},\infty} - \alpha_{i,\mathrm{sd}}), \tag{10}$$

$$\frac{d\alpha_{i,\mathrm{sa}}}{dt} = \frac{\phi}{\tau_{\mathrm{sa}}}(-\eta J_{i,\mathrm{sd}} - \gamma\alpha_{i,\mathrm{sa}}), \tag{11}$$

where τ_{Na}, τ_{K}, τ_{sd}, and τ_{sa} are constants.[31] The terms η and γ are related to the increase and decrease of the concentration of Ca^{2+} ions,[30] respectively, and ϕ represents a second temperature dependence of the model, given by

$$\phi = \phi_0^{(T-T_0)/\tau_0}. \tag{12}$$

$\alpha_{i,Na,\infty}$, $\alpha_{i,\mathrm{K},\infty}$, and $\alpha_{i,sd,\infty}$ are activation functions that depend on the potential of the membrane and it is described as

$$\alpha_{i,\mathrm{Na},\infty} = \frac{1}{1+\exp[-s_{\mathrm{Na}}(V_i - V_{0\mathrm{Na}})]}, \tag{13}$$

$$\alpha_{i,\mathrm{K},\infty} = \frac{1}{1+\exp[-s_{\mathrm{K}}(V_i - V_{0\mathrm{K}})]}, \tag{14}$$

$$\alpha_{i,\mathrm{sd},\infty} = \frac{1}{1+\exp[-s_{\mathrm{sd}}(V_i - V_{0\mathrm{sd}})]}. \tag{15}$$

s_{Na}, s_{K}, s_{sd}, $V_{0\mathrm{Na}}$, $V_{0\mathrm{K}}$, and $V_{0\mathrm{sd}}$ are constants as defined in Ref. 31, whose values are given in Table I.

The dynamic behavior of one single neuron obtained from the neuron model described by Eqs. (1)–(15) varies according to the temperature. For lower temperatures, the membrane potential has single periodical spikes, and for the higher temperatures, the membrane potential has a sequence of spikes followed by a quiescent period (burst behavior). Here, we use $T_0 = 50\,^{\circ}\mathrm{C}$ which is compatible with mammal temperatures range, $T \sim 37\,^{\circ}\mathrm{C}$ in Eq. (12).[34]

The coupling term $J_{i,coup}$, in Eq. (1) can be understood as an excitatory chemical synapse. In this way, the ith postsynaptic neuron receives signals from presynaptic neurons as proposed in Ref. 35

$$J_{i,\mathrm{coup}} = \frac{\varepsilon}{\zeta_{\mathrm{c,max}}}\sum_{j=1}^{N} e_{i,j} r_j (V_{\mathrm{syn}} - V_i), \tag{16}$$

where ε is the coupling parameter who controls the coupling intensity, $\zeta_{\mathrm{c,max}}$ is the normalization factor, set here as the number of connections of the most connected neuron. V_{syn} is the synaptic reversal potential (we use the value of 20 mV), $e_{i,j}$ represents the elements of the small-world connection matrix generated through Newmann-Watts construction,[25] using a probability of adding non-local connections $p = 0.001$.

Added to the model, r_j refers to chemical synapses, specifically the fraction of bound receptors available to receive a connection. We use the kinetic equation for temporal evolution of r_j proposed by Ref. 35,

$$\frac{dr_j}{dt} = \left(\frac{1}{\tau_r} - \frac{1}{\tau_d}\right)\frac{1-r_j}{1+\exp[-s_0(V_j - V_0)]} - \frac{r_j}{\tau_d}, \tag{17}$$

where s_0 is an unitary constant (1/mV), $V_0 = -20$ mV, $\tau_r = 0.5$ ms, and $\tau_d = 8$ ms and are model's constants.

To verify the general validity of our result we use another neuron model, the Hindmarsh-Rose model,[32] a set of three coupled differential equations which can reproduce the same bursting behavior of the more complex model of thermally sensitive neurons.[31] The time evolution of the three main variables of the Hindmarsh-Rose model, x_i (fast variable), y_i and z_i are given by

$$\frac{dx_i}{dt} = y_i - ax_i^3 + bx_i^2 - z_i + I + I_{i,\mathrm{coup}}, \tag{18}$$

$$\frac{dy_i}{dt} = c - dx_i^2 - y_i, \tag{19}$$

$$\frac{dz_i}{dt} = r[s(x_i - x_r) - z_i], \tag{20}$$

where a, b, c, d, r, s, x_r, and I are model's dimensionless parameters and $I_{i,\mathrm{coup}}$ is the chemical synaptic coupling term (analogous to $J_{i,\mathrm{coup}}$) and written as

$$I_{i,\mathrm{coup}} = \frac{\varepsilon}{\zeta_{\mathrm{c,max}}}\sum_{j=1}^{N} e_{i,j}\frac{(x_s - x_i)}{1+\exp[-\lambda(x_j - \beta_s)]}. \tag{21}$$

TABLE I. Parameter values of the neural dynamics models according to Ref. 31 (thermally sensitive model) and 32 (Hindmarsh-Rose model).

Thermally sensitive model				
Membrane capacitance	$C_{\mathrm{m}} = 1.0$ (μ Fcm^{-2})			
Maximum conductances (mS/cm^2)	$\bar{g}_{\mathrm{Na}} = 1.5$	$\bar{g}_{\mathrm{K}} = 2.0$	$\bar{g}_{\mathrm{sd}} = 0.25$	$\bar{g}_{\mathrm{sa}} = 0.4$
	$\bar{g}_{\mathrm{L}} = 0.1$			
Characteristic times (ms)	$\tau_{\mathrm{Na}} = 0.05$	$\tau_{\mathrm{K}} = 2.0$	$\tau_{\mathrm{sd}} = 10$	$\tau_{\mathrm{sa}} = 20$
Reversal potentials (mV)	$E_{\mathrm{Na}} = 50$	$E_{\mathrm{K}} = -90$	$E_{\mathrm{sd}} = 50$	$E_{\mathrm{sa}} = -90$
	$E_{\mathrm{L}} = -60$	$V_{0\mathrm{Na}} = -25$	$V_{0\mathrm{K}} = -25$	$V_{0\mathrm{sd}} = -40$
Other parameters	$\rho_0 = 1.3$	$\phi_0 = 3.0$	$T_0 = 50\,^{\circ}\mathrm{C}$	$\tau_0 = 10\,^{\circ}\mathrm{C}$
	$s_{\mathrm{Na}} = 0.25$ (mV^{-1})	$\eta = 0.012\ \mu$A	$\gamma = 0.17$	$s_{\mathrm{K}} = 0.25$ (mV^{-1})
	$s_{\mathrm{sd}} = 0.09$ (mV^{-1})	$T = 38\,^{\circ}\mathrm{C}$		
Hindmarsh-Rose model				
$a = 1$	$b = 3$	$c = 1$	$d = 5$	$s = 4$ $x_r = -8/5$ $s = 0.006$ $x_s = 2$ $\beta_s = 0$ $\lambda = 30$	

ε, $\zeta_{c,\max}$, and $e_{i,j}$ are parameters similar to those used in $J_{i,\text{coup}}$. x_s, λ, and β_s are constants related to the chemical synapses.

Concerning the topology characteristics, it is known that small-world networks have a small mean path length (L) and large clustering coefficient (C). In comparison to equivalent random networks, it is known that $L \sim L_{\text{rand}} \sim \ln(N)/\ln(n/N)$ and $C \gg C_{\text{rand}} \sim n/N^2$,[36,37] where N is the number of elements in the network, and n is the number of connections.[34,38,39] It is possible to define a merit coefficient $\sigma = \lambda_C/\lambda_L$, where $\lambda_L = L/L_{\text{rand}}$ and $\lambda_C = C/C_{\text{rand}}$ such that for a small-world network $\sigma > 1$. For our network with $N = 2000$ neurons, $p = 0.001$ and two-neighborhood results in $n = 9996$ connections. Numerical calculations lead to $L = 5.021$ and $C = 0.243$, and for a random equivalent network $L_{\text{rand}} \approx 4.724$ and $C_{\text{rand}} \approx 0.0025$. These results lead to $\sigma \sim 10^2$, which indicates the small-world topology.

To integrate the equations that compose both models and their related coupled equations, we use Adams' predictor corrector method[40] with an absolute tolerance less than 10^{-8}. Figures 1(a) and 1(b) (black lines) depict the membrane potential for both models, using the fixed set of parameter values depicted in Table I, (a) the fast variable of the thermally sensitive model, (V_i) with $T = 38\,^{\circ}\text{C}$ and (b) the fast variable of the Hindmarsh-Rose model, (x_i) with $I = 2.92$. Both models have the same dynamic behavior of bursting neurons.

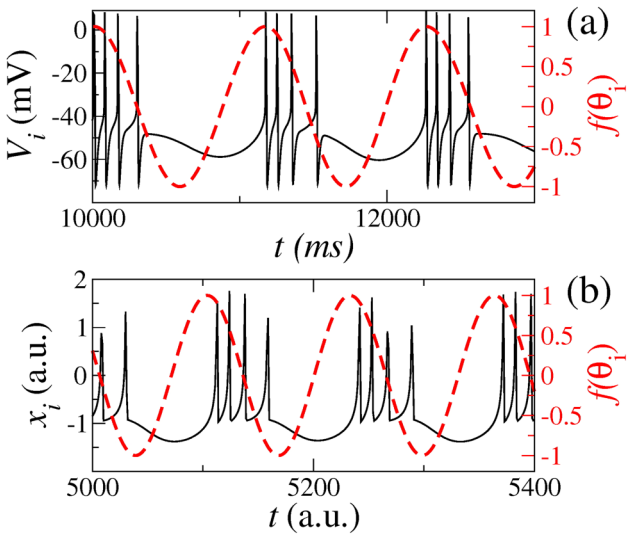

FIG. 1. (a) Time evolution of the dynamic behavior of the membrane potential, V_i for one single neuron of the Hodgkin-Huxley thermally sensitive model with $T = 38\,^{\circ}\text{C}$ (black line) and (b) the time evolution of the dynamics of the fast variable x_i of the Hindmarsh-Rose model with $I = 2.92$ (black line). In both cases, we use all the constants defined in Table I. The red dashed line is the function $f(\theta_j) = \cos(\theta_j)$ computed using Eq. (22) for each neuron model. At the beginning of the burst, $t = t_k$ the phase is a 2π multiple so $f(\theta_j) = 1$.

III. PHASE SYNCHRONIZATION AND RECURRENCE ANALYSIS

A characteristic of both bursting neurons network used in this work is the presence of PS. The sequence of bursting can be used to define a geometric phase for each neuron, $\theta_j(t)$, and used to quantify the phase synchronized behavior of the network. Each time a new burst occurs, $\theta_j(t)$ is increased by 2π such that a continuous time varying phase is defined using a simple linear interpolation

$$\theta_j(t) = 2\pi k_j + 2\pi \frac{t - t_{k,j}}{t_{k+1,j} - t_{k,j}}, \quad t_{k,j} \le t < t_{k+1,j}, \tag{22}$$

where k_j is the kth burst of the jth neuron, t is the current time, and $t_{k,j}$ is the time for which the jth neuron starts the kth burst. In Fig. 1, the black solid lines depict the bursting fast variables of the thermally sensitive Hodgkin-Huxley, panel (a) and Hindmarsh-Rose, panel (b) models. The dashed red lines display the harmonic function $f(\theta_j) = \cos\theta_j(t)$. Each time a new burst starts the cosine amplitude reaches 1, so it can be used to compute the Kuramoto order parameter

$$R(t) = \left| \frac{1}{N} \sum_{j=1}^{N} e^{i\theta_j(t)} \right| \tag{23}$$

to quantify PS states of the network.[2,4] In Eq. (23), N is the network size and θ_j is the phase of the jth neuron, defined by Eq. (22). The temporal mean value of the order parameter is defined as

$$\langle R \rangle = \frac{1}{M} \sum_{j=1}^{M} R(\tau_j), \tag{24}$$

being $\tau_1 = t_i, \tau_2 = t_i + h, \ldots, \tau_M = t_f$, where $h = 0.01$. $\langle R \rangle \approx 1$ for all time intervals, means that the network has reached a globally stable phase synchronized state.

The use of $\langle R \rangle$ to quantify PS depends on the evaluation of the temporal signal of each neuron. A simpler way to get useful information about the phase synchronized states consists of measuring the mean field of the network, the Mean Field Potential (MFP) of the network,[41] defined by

$$\overline{V} = \frac{1}{N} \sum_{i=1}^{N} V_i, \tag{25}$$

for the Hodgkin-Huxley model, and

$$\overline{x} = \frac{1}{N} \sum_{i=1}^{N} x_i, \tag{26}$$

for the Hindmarsh-Rose model.

Figure 2 depicts the characteristics of the MFP $\overline{V}$ of the thermally sensitive neural network model, for distinct values of the coupling parameter: (a) $\varepsilon = 0.010$, an anomalous phase synchronized case occurring for a very weak coupling parameter amplitude ($\approx 1/8$ of the coupling value obtained for similar globally stable synchronization), (b) $\varepsilon = 0.016$, an unsynchronized case and (c) $\varepsilon = 0.080$, a globally stable phase synchronized state. The anomalous PS depicts temporal patterns of the MFP [Fig. 2(a)] very similar to those observed for normal PS [Fig. 2(c)], sharing almost all its properties but occurring for coupling parameter eight times lower. The occurrence of phase synchronized states for such a very weak coupling regime justify the adjective anomalous.

The MFP reflects the properties of (un)synchronization states as shown in Fig. 2, suggesting that a deep statistical

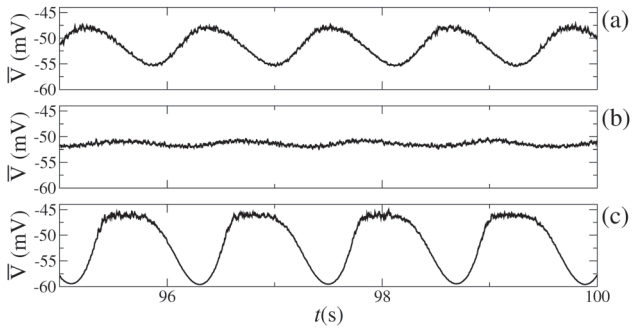

FIG. 2. Mean Field Potential $\overline{V}$ for a $N = 2000$ thermally sensitive neural network with $T = 38\,^{\circ}$C, in (a) $\varepsilon = 0.010$, (b) $\varepsilon = 0.016$, and (c) $\varepsilon = 0.080$.

analysis of the signal can result in a tool to quantify asymptotic states depicted by networks. In fact, it was shown that recurrence analysis based on MFP signals shows similar information to those reported using the order parameter, Eq. (24), to quantify the transition to PS of networks.[27,28]

Recurrence properties of systems were first developed by the pioneering work of Poincaré,[42] but a useful way to visualize the recurrent properties of systems was developed much later, with the description of recurrence plots (RPs) and its quantifiers.[43,44] A RP is a matrix composed by "zeros" and "ones." One (zero) refers to a pair of recurrent (non-recurrent) points, (i,j), $i = 1,\ldots,N$. $j = 1,\ldots,N$, in the time series. Mathematically, the recurrence matrix, $\mathbf{R}_{ij}$ is defined as

$$\mathbf{R}_{ij}(\delta) = \Theta(\delta - |\mathbf{x}_i - \mathbf{x}_j|), \mathbf{x}_i \in \mathbb{R}, \quad i,j = 1,2,\ldots,L, \quad (27)$$

where L is the size of the analyzed time series, δ the threshold to consider two points in phase space as recurrent, and Θ is the Heaviside function.

An important characteristic of RP that is used to get information about PS of networks is the presence of diagonal lines formed from recurrence points. The presence of diagonal lines on a RP implies the existence of a set of initial conditions that evolutes in time in a similar way. Based on these ideas, it is defined the determinism Δ,[44] a recurrence quantifier which measures the fraction of recurrence points forming diagonal lines in a RP and given by

$$\Delta(\ell_{\min},\delta) = \frac{\sum_{\ell=\ell_{\min}}^{L} \ell P(\ell,\delta)}{\sum_{\ell=1}^{L} \ell P(\ell,\delta)}, \quad (28)$$

where $P(\ell,\delta)$ is the probability distribution function of diagonal lines with length ℓ present in the RP, $\ell_{\min}$ is the threshold which defines the minimum number of points characterizing a diagonal line. The mean value of $\Delta(t)$ over a time interval $t_f - t_i$ is given by

$$\langle\Delta\rangle = \frac{1}{M}\sum_{j=1}^{M}\Delta(\tau_j), \quad (29)$$

being $\tau_1 = t_i, \tau_2 = t_i + h, \ldots, \tau_M = t_f$, where $h = 0.01$.

Throughout this paper, for the thermally sensitive model, $\Delta(t)$ is computed using a moving window of size $L = 10\,000$, representative of ≈ 10 s of data and enclosing ≈ 8 bursts. To compute the recurrence matrix, we set usual values for $\ell_{\min} = 50$ and $\delta = 0.11$.[44] Similar values are used for the Hindmarsh-Rose model, $L = 10\,000$ and $\delta = 0.15$. In this model, we set $\ell_{\min} = 10$ due to the distinct time scale of the problem.

IV. RESULTS

Considering the thermally sensitive and Hindmarsh-Rose models of neuron dynamics, we simulate neural small-world networks composed of $N = 2000$ identical neurons subjected to excitatory coupling scheme, representing chemical synapses between neurons.[25] As local connections, it is added two nodes away neighbors, totalizing 8000 connections. The probability of adding non-local connections is set to $p = 0.001$, resulting in ≈ 2000 shortcuts in the networks. For the thermally sensitive neuron model, a transient time $t_i = 50$ s is considered and the final time is set to $t_f = 100$ s. An equivalent interval of time is used for the Hindmarsh-Rose model, given enough information to evaluate the determinism, as defined by Sec. III.

The action potential dynamics of a thermally sensitive neuron depends on the temperature T[31] and can be used to identify distinct properties of the network when this parameter is varied. In fact, recent studies show the existence of a neuropathology originated from changes on the temperature of the neural system, called "hot-water epilepsy."[45,46] The increase of temperature of neurons may induce events of epilepsy,[45] and in some cases, the seizures are related to anomalous PS.[10]

To make clear, the dependence of the anomalous PS depicted by thermally sensitive neurons network against changes on the temperature and coupling parameter, Figs. 3(a) and 3(b) shows the mean values of the order parameter $\langle R\rangle$, computed from the individual signals of all neurons and the mean values of the determinism $\langle\Delta\rangle$, computed from the MFP of the network Eq. (25), as functions of the temperature T, for a large interval of the coupling parameter ε. For low temperatures $T < 38\,^{\circ}$C and weak a coupling parameter, $\varepsilon < 0.02$, the network is unsynchronized. As the coupling increases and considering a low $T < 38\,^{\circ}$C temperature, the network starts to synchronize, reaching a globally stable synchronized state, describing a typical sigmoid curve in the parameter spaces $(\langle R\rangle \times \varepsilon)$ or $(\langle\Delta\rangle \times \varepsilon)$. This behavior is similar to those observed for non-inertial Kuramoto oscillators and also for some chaotic coupled oscillator.[6,8,20,27,28,34] For this interval of temperatures, anomalous PS is not observed.

For temperatures $T > 38\,^{\circ}$C, the network starts to display an anomalous PS occurring for lower coupling parameter, $\varepsilon < 0.02$, regime. For temperatures greater than $T = 39\,^{\circ}$C, the level of anomalous PS is as high as the asymptotic globally stable synchronized state that occurs for much higher coupling parameters. As extensively studied in Refs. 27 and 28, for these situations, an increase of the coupling parameter, initially makes the network to desynchronize, and a further increase of the coupling parameter leads the network to the globally stable synchronized state.

A closer analysis of Figs. 3(a) and 3(b) shows the usefulness of the determinism to characterize the transition to PS of networks. Observe that all information about the transition to PS is visible in both panels, but the determinism is obtained

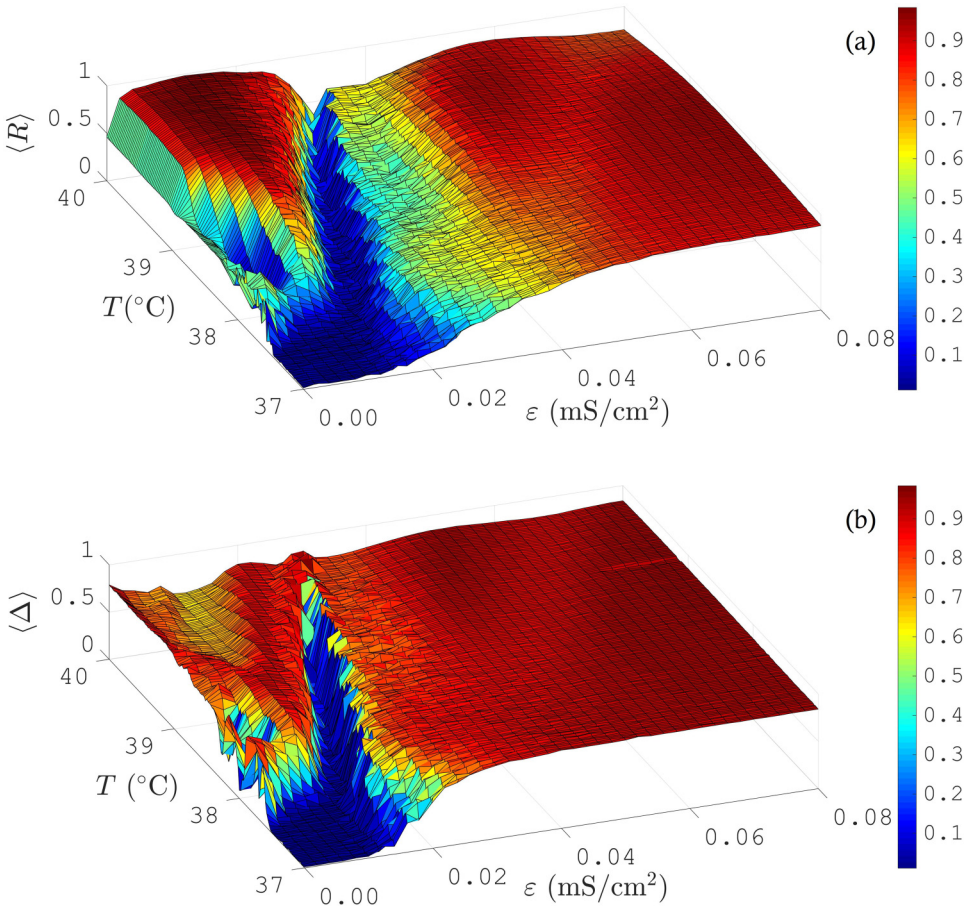

FIG. 3. (a) $\langle R \rangle$ and $\langle \Delta \rangle$ as functions of ε and the temperature T. For low temperatures, the network does not display anomalous PS. As the temperature increases, $T > 38\,^{\circ}\mathrm{C}$, anomalous PS starts to occur.

using just MFP, a much more accessible data in almost all experimental situations.

In order to understand the occurrence of the anomalous PS, we analyze the individual behavior of the neurons, defining the Inter-Burst-Intervals (*IBI*s), i.e., the time between two consecutive bursts, $IBI = t_{k+1} - t_k$ for *one isolated or coupled neuron*. Figures 4(a) and 4(b) depict the bifurcation diagram of *IBI* as a function of the temperature T, measured in °C and for an isolated (a) and coupled neuron (b) of the thermally sensitive model, considering $\varepsilon = 0.01$ (mS/cm^2). Observe that for higher temperatures, $T > 39\,^{\circ}\mathrm{C}$, the *IBI* are periodic for the isolated neuron (a), and depict just a small dispersion around those periodic values when the effect of the coupling is taken into account (b), since for these regimes the network is just weakly coupled. For $38\,^{\circ}\mathrm{C} < T < 39\,^{\circ}\mathrm{C}$, the isolated neuron has a 2-period *IBI* and, for the coupled neuron *IBI* suffer just a slightly larger dispersion. For lower temperatures $T < 38\,^{\circ}\mathrm{C}$, the *IBI* of the neuron has a great variability due to the intrinsic chaotic dynamics of the isolated neuron, as well as due to the effect of the coupling over the already chaotic neuron. Such behavior of the *IBI* variability correlates very well with the existence of anomalous PS of the network, as it is seen in Fig. 3. A small variability of the *IBI* of the neurons leads the network to display anomalous PS. As observed in Figs. 3 and 4, the lower the variability of the *IBI*, the greater the anomalous PS.

To investigate further the interdependent relation of the variability of the *IBI* of neurons and the anomalous PS of the network, we promote an external perturbation on the thermally sensitive neuron networks and also on a second network based on Hindmarsh-Rose neuron model.

Motivated by experimental setups,[47–49] we establish a protocol of perturbation of the network consisting in applying an external pulsed current in the main equation of the neuron

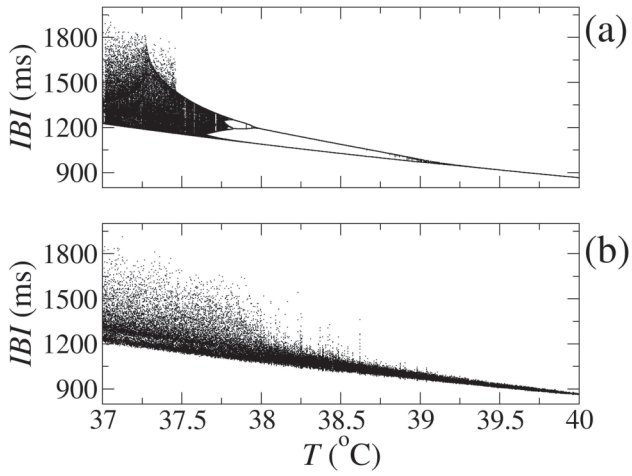

FIG. 4. *IBI* as a function of the temperature T measured in °C for (a) an isolated thermally sensitive neuron and (b) coupled neuron. Observe that the coupling just imposes a small dispersion on the periodic IBI. For lower temperatures, $T < 38\,^{\circ}\mathrm{C}$, the variability of the IBI increases due to the chaotic behavior of the isolated neuron. $\varepsilon = 0.01$ (mS/cm^2).

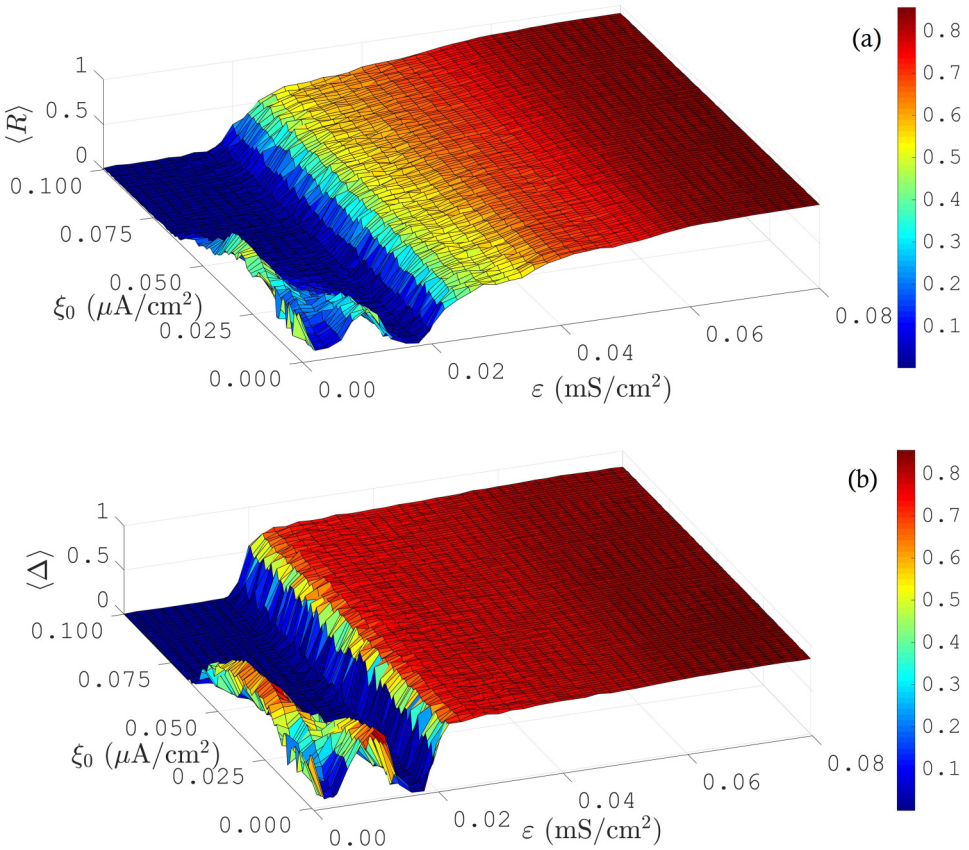

FIG. 5. $\langle R\rangle$ (a) and $\langle \Delta\rangle$ (b) as functions of ε for distinct values of the external $\nu = 150$ Hz pulsed current amplitude, ξ_0 as defined in Eq. (31). As the pulsed current amplitude grows, the anomalous PS of the network is depleted.

model, Eq. (1).

$$C_{\rm m}\frac{dV_i}{dt} = -J_{i,\rm Na} - J_{i,\rm K} - J_{i,\rm sd} - J_{i,\rm sa} - J_{i,\rm L} + J_{i,\rm coup} + \xi(t), \tag{30}$$

where $\xi(t)$ is an external high frequency rectangular waveform current measured in μA/cm^2[28] and given by

$$\xi(t) = \frac{\xi_0}{2} + \sum_{n=1,3,\ldots}^{\infty} \frac{2\xi_0}{n\pi}\sin(n\pi\nu t), \tag{31}$$

ν and ξ_0 are the frequency and amplitude of the pulse, respectively. Such an external amplitude current does not alter the natural bursting dynamics of the neuron, but similarly to the changes promote by the temperature T, the application of the electromagnetic pulses changes the *IBI* of the neuron.

We consider a thermally sensitive neuron network for $T = 38\,^{\circ}$C, but subjected to an external pulsed current given by Eq. (31) applied to every neuron in the network. Figures 5(a) and 5(b) display the dependence of $\langle R\rangle$, (a), and $\langle\Delta\rangle$, (b), as functions of ξ_0, for a large interval of the coupling, ε. We fix the value of $\nu = 150$ Hz since traditional experiments show that only high frequency ($\nu > 100$ H) can reverse undesirable motor symptoms.[50,51] In fact, our simulations show that low frequencies ($\nu < 50$ Hz) accentuate the anomalous PS.

For a low amplitude of the external current, $\xi_0 < 0.04\,\mu$A/cm^2, the network is partially synchronized considering just low coupling values. It is expected since it reflects just a small perturbation over the anomalous PS regime that occurs for the network for $T = 38\,^{\circ}$C. For larger amplitudes of the external pulsed current, $\xi_0 > 0.04$, the anomalous PS is completely depleted. The pulsed external current promotes the complete desynchronization of the network for weak coupling regimes. Observe also that the (expected) globally stable PS states occurring for higher coupling values do not suffer any changes due to the external pulsed current that acts selectively on the anomalous PS regime.

Figure 6 shows the bifurcation diagram of the *IBI* of isolated (a) and coupled neurons (b) of the thermally sensitive neurons, as a function of the amplitude of the external pulse ξ_0 for a fixed frequency $\nu = 150$ Hz. Again, we have the effect of such a growing amplitude of the external pulsed

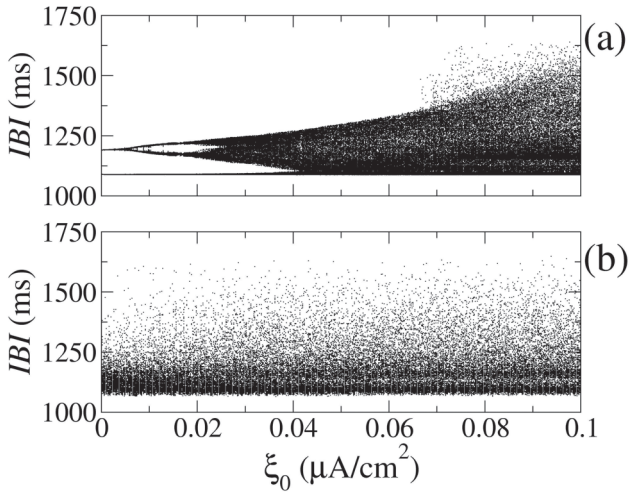

FIG. 6. *IBI* as a function of the amplitude of the external pulsed current ξ_0 measured in μA/cm^2 for an isolated (a) and coupled (b) thermally sensitive neuron for $T = 38\,^{\circ}$C and fixed frequency, $\nu = 150$ Hz of the perturbed current. The variability of IBI grows as a function of the external pulsed current amplitude, ξ_0 grows.

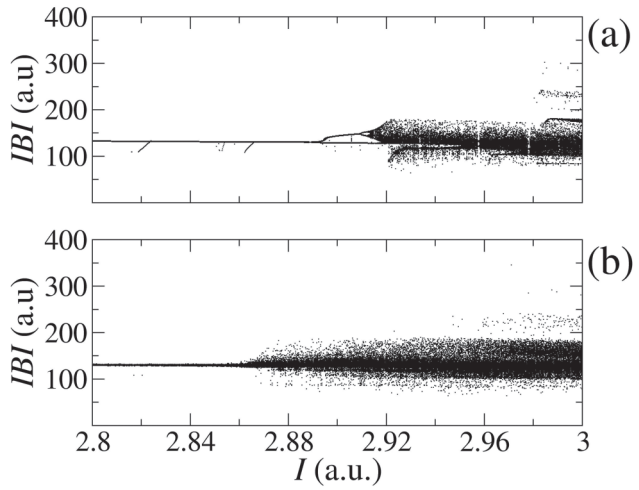

FIG. 7. Bifurcation diagram of *IBI* as a function of I for an isolated Hindmarsh-Rose neuron Eqs. (18)–(20), and fixed parameters are shown in Table I. For $I < 2.9$, the *IBI* are periodic, for $2.9 < I < 2.92$, it has a 2-period behavior and $I > 2.92$ the variability increases. (b) For the coupled neuron, $\varepsilon = 0.1$, it is observed an increase in the variability as a function of I.

perturbation promotes changes in the individual dynamics of the neuron. For amplitudes ($\xi_0 < 0.01$), the pulsed external current does not destroy small variability of an isolated neuron that has three characteristic *IBI* values subjected to a small fluctuation due to the external perturbation. If the coupling with the entire network is added to the behavior of the neuron, the *IBI* values keep a strong component distributed over the former three periodic values depicted by the individual neuron, but in this case, larger values of *IBI* are sporadically observed. For large perturbation amplitudes $\xi_0 > 0.02$, the variability grows as a function of the external pulsed amplitude such that for $\xi_0 > 0.04$, the *IBI* of the isolated neuron reach a "continuous" range between 900 and 1250 ms. For the coupled neuron dynamics, it is possible to observe that the *IBI* around 1100 ms starts to diminish, spreading its values over a larger interval of time. Figure 5 suggests that an external pulsed amplitude larger than $\xi_0 > 0.04$ imposes enough variability to the individual neurons, depleting the anomalous PS.

The effect of the external pulsed current over the intrinsic dynamics of each neuron corroborates the idea that the collective dynamic behavior of the network is influenced by the individual behavior of single neurons. To make the interdependent relation between the individual neuron variability and the collective behavior of a network even clearer, we have studied the effect of the external perturbation current, I, described by Eq. (18) on a second neuron model, namely, the simpler and dimensionless Hindmarsh-Rose model,[32] where all fixed parameters are described in Table I. For those parameters, the fast variable x_i reproduces bursting behavior in a similar way as the membrane potential of the thermally sensitive neuron model does, as observed in Figs. 1(a) and 1(b).

Figure 7(a) shows the bifurcation diagram of *IBI* of an isolated neuron for the Hindmarsh-Rose model, as a function of the external current, I for the isolated neuron (a) and for

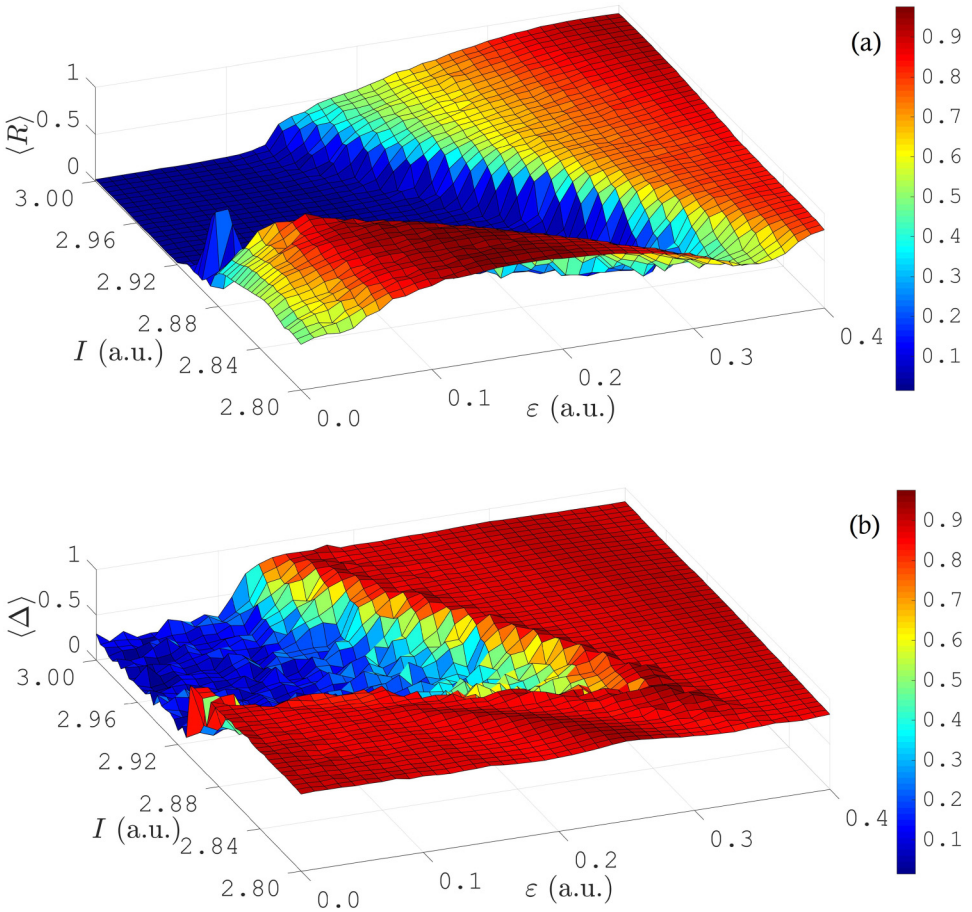

FIG. 8. $\langle R \rangle$ (a) and $\langle \Delta \rangle$ as functions of ε for distinct values of I for a small-world neural network with $N = 2000$ Hindmarsh-Rose neurons coupled with a chemical synapse given by Eq. (21). For $I < 2.92$, the network has anomalous PS. For $I > 2.92$, the anomalous PS is depleted due to the increase of variability of IBI of individual neurons, as observed in Fig. 7.

the coupled neuron (b), for a coupling strength $\varepsilon = 0.1$ in Eq. (21). Observe that for the coupled neuron, a second current, I_{coup}, Eq. (21) is added to the external current term in Eq. (18). So the observed shift to the left of the bifurcation diagram is expected. For $I < 2.9$, the neuron has a periodic *IBI* suffering a small variability. For $2.9 < I < 2.92$, the IBI of the neurons has its variability increased, displaying a 2-period *IBI*. For these regimes, we expect that the Hindmarsh-Rose network depicts anomalous PS. We also expect that, for $I > 2.92$, the anomalous synchronized states should diminish or be completely depleted since the variability of *IBI* of the Hindmarsh-Rose neurons increases. At this point, we expect a transition from an anomalous phase synchronized state for lower values of I, to the absence of anomalous PS for higher values of I, in a similar way as it occurs for the thermally sensitive neurons and depicted in Figs. 3 (temperature variation) and 5 (external pulsed current).

Figures 8(a) and 8(b) display the dependence of $\langle R \rangle$ (a) and $\langle \Delta \rangle$ (b), over I for a large interval of the coupling parameter for a network of $N = 2000$ Hindmarsh-Rose neurons, and we use the MFP defined in Eq. (26) to evaluate the determinism $\langle \Delta \rangle$. As predicted by our consideration based on the bifurcation diagram of *IBI*, for $I < 2.92$, the network does display anomalous PS, diminishing for larger values of I and disappearing for $I > 2.92$, a critical coupling parameter value for which the larger variability of individual neurons avoids anomalous phase synchronized states.

V. CONCLUSION

We have shown the existence of an interdependent relation between the anomalous PS depicted by networks under small-world topology, and subject to weak coupling to the individual variability of single neurons of the network.

For both networks dealt here the behavior of each neuron results from the complex interplay between the natural diffusive dynamics of each node and the collective behavior imposed by the coupling strength. In this scenario, one should expect a monotonous dependence of the synchronization strength on the coupling parameter. In fact, this is the standard scenario observed in many cases described in the literature. But contrarily, the thermal sensitive neuron, derived from the Hodgkin-Huxley model and the Hindmarsh-Rose neuron model exhibit a first branch of synchronized dynamics even for very weak coupling strength, characterizing a non-monotonous dependence of the synchronization strength on the coupling strength when subjected to similar small-world network topologies and chemical synapses.

A more heterogeneous distribution of individual behaviors of neurons is responsible for the spontaneous collapse of anomalous PS. This scenario resembles explosive (de)synchronization phenomenon, emerging from the interactions of distinct dynamical states on a network.[52] The presence of such an easy (allowed by just small changes in the coupling strength) switchlike transition may be related to the ability of the network to quickly switch between two different states, the phenomenon observed in many natural networks including the brain.[53,54]

The individual behaviors of neurons are evaluated using the variability of the Inter-Burst-Interval, *IBI*. We observe that smaller variability implies the presence of anomalous PS of the network. In general, the interdependent relation, the smaller variability of neuron dynamics, the greater anomalous PS, is observed for both simulated network.

We have demonstrated a clear relation between the individual dynamics of a neuron and the complex global behavior of the network. On the other hand, the complexity imposed by the collective phenomenon is also important. An interplay between the individual and collective behaviors brings the final dynamics of the network. The origin of this phenomenon is much better understood when we analyze both contributions. The interdependent relation suggests that for neurons depicting small variability, the PS process occurs in a similar way as the process of phase locking occurring in regular (non-chaotic) oscillators. It is known that for the case of completely ordered oscillators, the phase locking process does not display a clear threshold value, starting as soon as the coupling exists. Otherwise, the PS of chaotic oscillators displays a threshold value for the coupling, such that the anomalous PS results from an interplay between the tendency of uncoupled regular neurons to display (phase) mode coupling under small coupling regimes, and the presence of a finite threshold for PS when the neurons display an already chaotic behavior. The former behavior is possible since even small amplitude couplings induce some chaotic dynamics into the neurons. So the effect of the weak coupling is to turn the former regular neurons into chaotic ones at the same time that it imposes a gradual phase synchronized dynamics into the network.

To test the hypothesis, we have perturbed the network making changes on a parameter of the models or introducing an external current on the network. For all situations analyzed, the dependence of the anomalous PS over the presence of a small variability of neurons (just weakly chaotic) is observed. When the neuron has a large variability of *IBI* (strongly chaotic even for weak coupling), the transition between desynchronized to phase synchronized states of the network follows the traditional route depicting a sigmoid curve when the coupling parameter is varied.

The knowledge about a close relation between the individual neuron variability and the collective behavior of the network can be directly applied to the suppression (or control) of PS of the network since it can target ways to control the variability of neurons as a starting point to obtain collective changes in the dynamics of the network.

Finally, we show that all the characteristics of the transition from desynchronized to phase synchronized network, as the coupling parameter is varied, can be detected with the use of a recurrence quantifier, the determinism, which in this case, measures the coherence of the mean field potential (MFP) of the network as the coupling is varied. The MFP is a much more natural measure of the network dynamics and our results show that we can identify PS in a way as effective as the use of the mean order parameter does, but without the necessity to evaluate individual signals of all neuron signals of the network. The MFP is a macroscopic measure, and can be easily calculated, and our results show that the use of

the determinism over MFP reflects the PS behavior as well as properties of the transition regime.

ACKNOWLEDGMENTS

The authors acknowledge the financial support of Conselho Nacional de Desenvolvimento Científico e Tecnológico, CNPq - Brazil, through fellowship and Grant No. 302785/2017-5, and Coordenação de Aperfeiçoamento de pessoal de Nível Superior, CAPES, through fellowship and Project No. 88881.119252/2016-01.

[1]B. Blasius, A. Huppert, and L. Stone, Nature **399**, 354EP (1999).
[2]Y. Kuramoto, Phys. D Nonlinear Phenom. **50**, 15 (1991).
[3]N. F. Rulkov, M. M. Sushchik, L. S. Tsimring, and H. D. Abarbanel, Phys. Rev. E **51**, 980 (1995).
[4]Y. Kuramoto, *Chemical Oscillations, Waves, and Turbulence* (Springer Science & Business Media, 2012). Vol. 19.
[5]N. F. Rulkov, Phys. Rev. Lett. **86**, 183 (2001).
[6]C. A. S. Batista, A. M. Batista, J. A. C. De Pontes, R. L. Viana, and S. R. Lopes, Phys. Rev. E **76**, 016218 (2007).
[7]I. Belykh, E. de Lange, and M. Hasler, Phys. Rev. Lett. **94**, 188101 (2005).
[8]C. A. S. Batista, E. L. Lameu, A. M. Batista, S. R. Lopes, T. Pereira, G. Zamora-López, J. Kurths, and R. L. Viana, Phys. Rev. E **86**, 016211 (2012).
[9]C. Hammond, H. Bergman, and P. Brown, Trends. Neurosci. **30**, 357 (2007).
[10]F. Mormann, K. Lehnertz, P. David, and C. E. Elger, Phys. D: Nonlinear Phenom. **144**, 358 (2000).
[11]B. Percha, R. Dzakpasu, M. Żochowski, and J. Parent, Phys. Rev. E **72**, 031909 (2005).
[12]E. R. Kandel, J. H. Schwartz, T. M. Jessell, S. A. Siegelbaum, A. J. Hudspeth *et al. Principles of Neural Science* (McGraw-Hill, New York, 2000) Vol. 4.
[13]J. G. Nicholls, A. R. Martin, B. G. Wallace, and P. A. Fuchs, *From Neuron to Brain* (Sinauer Associates Sunderland, MA, 2001), Vol. 271.
[14]E. Bullmore, and O. Sporns, Nat. Rev. Neurosci. **10**, 186 (2009).
[15]S. H. Strogatz, Nature **410**, 268 (2001).
[16]D. S. Bassett, and E. D. Bullmore, Neuroscientist. **12**, 512 (2006).
[17]W. Zhou, J. Yang, L. Zhou, and D. Tong, *Stability and Synchronization Control of Stochastic Neural Networks* (Springer, Berlin, 2015).
[18]V. M. Eguiluz, D. R. Chialvo, G. A. Cecchi, M. Baliki, and A. V. Apkarian, Phys. Rev. Lett. **94**, 018102 (2005).
[19]R. C. Budzinski, B. R. R. Boaretto, K. L. Rossi, T. L. Prado, J. Kurths, and S. R. Lopes, Phys. A: Stat. Mech. Appl. (2018).
[20]C. A. S. Batista, R. L. Viana, F. A. S. Ferrari, S. R. Lopes, A. M. Batista, and J. C. P. Coninck, Phys. Rev. E **87**, 042713 (2013).
[21]C. Park, R. M. Worth, and L. L. Rubchinsky, J. Neurophysiol. **103**, 2707 (2010). j00724-9[PII].
[22]C. Park, R. M. Worth, and L. L. Rubchinsky, Phys. Rev. E **83**, 042901 (2011).
[23]L. R. Varshney, B. L. Chen, E. Paniagua, D. H. Hall, and D. B. Chklovskii, PLoS. Comput. Biol. **7**, 1 (2011).
[24]Y. He, Z. J. Chen, and A. C. Evans, Cereb. Cortex **17**, 2407 (2007).
[25]M. E. J. Newman, and D. J. Watts, Phys. Rev. E **60**, 7332 (1999).
[26]B. Blasius, E. Montbrió, and J. Kurths, Phys. Rev. E **67**, 035204 (2003).
[27]R. C. Budzinski, B. R. R. Boaretto, T. L. Prado, and S. R. Lopes, Phys. Rev. E **96**, 012320 (2017).
[28]B. R. R. Boaretto, R. C. Budzinski, T. L. Prado, J. Kurths, and S. R. Lopes, Phys. A: Stat. Mech. Appl. **497**, 126–138 (2018).
[29]A. L. Hodgkin, and A. F. Huxley, J. Physiol. (Lond.) **117**, 500 (1952).
[30]P. R. Shorten, and D. J. N. Wall, Bull. Math. Biol. **62**, 695 (2000).
[31]H. A. Braun, M. T. Huber, M. Dewald, K. Schäfer, and K. Voigt, Int. J. Bifurcat. Chaos **8**, 881 (1998).
[32]J. L. Hindmarsh, and R. M. Rose, Proc. R. Soc. Lond. B: Biol. Sci. **221**, 87 (1984).
[33]A. Rinberg, A. L. Taylor, and E. Marder, PLoS. Comput. Biol. **9**, e1002857 (2013).
[34]T. L. Prado, S. R. Lopes, C. A. S. Batista, J. Kurths, and R. L. Viana, Phys. Rev. E **90**, 032818 (2014).
[35]A. Destexhe, Z. F. Mainen, and T. J. Sejnowski, Neural. Comput. **6**, 14 (1994).
[36]P. Erdös, and A. Rényi, Publ. Math. (Debrecen) **6**, 290 (1959).
[37]P. Erdös, and A. Rényi, Publ. Math. Inst. Hung. Acad. Sci. **5**, 17 (1960).
[38]R. Albert, and A.-L. Barabási, Rev. Mod. Phys. **74**, 47 (2002).
[39]N. Boccara, *Modeling Complex Systems* (Springer Science & Business Media, 2010).
[40]S. D. Cohen, A. C. Hindmarsh, P. F. Dubois, *et al.* Comput. Phys. **10**, 138 (1996).
[41]G. Buzsáki, C. A. Anastassiou, and C. Koch, Nature Rev. Neurosci. **13**, 407 (2012).
[42]H. Poincaré, Acta Math. **13**, 1 (1890).
[43]J. P. Eckmann, S. O. Kamphorst, and D. Ruelle, EPL (Europhys. Lett.) **4**, 973 (1987).
[44]N. Marwan, M. C. Romano, M. Thiel, and J. Kurths, Phys. Rep. **438**, 237 (2007).
[45]T. Morimoto, T. Hayakawa, H. Sugie, Y. Awaya, and Y. Fukuyama, Epilepsia **26**, 237 (1985).
[46]P. Satishchandra, A. Shivaramakrishana, V. G. Kaliaperumal, and B. S. Schoenberg, Epilepsia **29**, 52 (1988).
[47]N. Grossman, D. Bono, N. Dedic, S. B. Kodandaramaiah, A. Rudenko, H.-J. Suk, A. M. Cassara, E. Neufeld, N. Kuster, L.-H. Tsai, A. Pascual-Leone, and E. S. Boyden, Cell **169**, 1029 (2017).
[48]A. L. Benabid, P. Pollak, D. Gao, D. Hoffmann, P. Limousin, E. Gay, I. Payen, and A. Benazzouz, J. Neurosurg. **84**, 203 (1996).
[49]D.-B. S. for Parkinson's Disease Study Group *et al.*, N. Engl. J. Med. **345**(13), 956–963 (2001).
[50]G. C. McConnell, R. Q. So, J. D. Hilliard, P. Lopomo, and W. M. Grill, J. Neurosci. **32**, 15657 (2012).
[51]J. S. Perlmutter, and J. W. Mink, Annu. Rev. Neurosci. **29**, 229 (2006).
[52]V. Nicosia, P. S. Skardal, A. Arenas, and V. Latora, Phys. Rev. Lett. **118**, 138302 (2017).
[53]G. Deco, V. K. Jirsa, and A. R. McIntosh, Trends. Neurosci. **36**, 268 (2013).
[54]E. A. Martens, S. Thutupalli, A. Fourrière, and O. Hallatschek, Proc. Natl. Acad. Sci. **110**, 10563 (2013).